Modeling and Simulation in Science, Engineering and Technology

Mathematical Modeling of Biological Systems, Volume I

Cellular Biophysics, Regulatory Networks, Development, Biomedicine, and Data Analysis

Andreas Deutsch
Lutz Brusch
Helen Byrne
Gerda de Vries
Hanspeter Herzel
Editors

Birkhäuser
Boston • Basel • Berlin

18

Mathematical Modelling of Vascular Tumour Growth and Implications for Therapy

Jasmina Panovska,[1] Helen M. Byrne,[2] and Philip K. Maini[3]

[1] Chemical Engineering, Heriot-Watt University, Riccarton Campus, Edinburgh, EH14 4AS; J.Panovska@hw.ac.uk
[2] Centre for Mathematical Medicine, Division of Applied Mathematics, School of Mathematical Sciences, University of Nottingham, Nottingham, NG7 2RD; Helen.Byrne@maths.nottingham.ac.uk
[3] Centre for Mathematical Biology, Mathematical Institute, Oxford University, Oxford, OX1 3LB; maini@maths.ox.ac.uk

Summary. In this chapter we briefly discuss the results of a mathematical model formulated in [22] that incorporates many processes associated with tumour growth. The deterministic model, a system of coupled non-linear partial differential equations, is a combination of two previous models that describe the tumour-host interactions in the initial stages of growth [11] and the tumour angiogenic process [6]. Combining these models enables us to investigate combination therapies that target different aspects of tumour growth. Numerical simulations show that the model captures both the avascular and vascular growth phases. Furthermore, we recover a number of characteristic features of vascular tumour growth such as the rate of growth of the tumour and invasion speed. We also show how our model can be used to investigate the effect of different anti-cancer therapies.

Key words: Vascular tumours, angiogenesis, hypoxia, anti-cancer therapy.

18.1 Introduction

Tumour growth is a complex process that involves a sequence of well-orchestrated events. These characterise the initial avascular phase of growth, the angiogenesis that enables the tumour to become vascularised and the vascular phase of growth. During the early stages of growth, oxygen is delivered to the tumour cells via diffusion from nearby blood vessels and the tumour cells proliferate rapidly and consume more oxygen than the host cells [7]. Due to the diffusion-limited supply of oxygen such growth is limited in size [31]. To grow larger the tumour must undergo a cascade of processes that include the secretion of tumour angiogenic factors, such as vascular endothelial growth factor (VEGF). VEGF stimulates the formation of a tumour-specific vascular network from the host vessels. Upon successful vascularisation oxygen is rapidly supplied to the tumour and it can grow larger.

Within the last three decades a number of mathematical models for tumour growth have been developed as part of the quest to understand tumour growth dynamics. Most of these models focus on one particular aspect, for example, avascular growth (e.g., [27,32]), tissue-tissue interactions (e.g., [11,28]), angiogenesis (e.g., [1,6,21]) or vascular tumour growth (e.g., [4,5,14,18]). However, if we wish to compare and contrast the effectiveness of different treatment protocols via mathematical modelling, we need a model that integrates several key processes that occur during tumour growth. A first attempt at deriving such a model was made by de Angelis and Preziosi [8]. They developed a model to describe the evolution of tumour growth from the avascular stage to the vascular stage through the angiogenic process. The model was able to predict the formation of necrotic regions, the control of mitosis by the presence of an inhibitory factor, the angiogenesis process with proliferation of capillaries just outside the tumour surface and the regression of the tumour and the angiogenic capillaries when angiogenesis was controlled or inhibited. Here we briefly describe an extended model to the one in [8] by including the density of the healthy host cells in the system, and we also model two distinct components of the vasculature, distinguishing between capillary tips and blood vessels. We refer the reader to [22] for full details. In Section 18.2, we present the model equations. In Section 18.3 we illustrate the types of behaviour that the model yields when formulated on a one-dimensional spatial domain. The potential use of our model for testing anti-tumour drug protocols is illustrated in Section 18.4. We present our conclusions and comment on future research directions in Section 18.5.

18.2 Model Formulation

The model we develop comprises a system of non-linear partial differential equations and aims to reproduce the animal chamber experiments of Gimbrone et al. [12] and Muthukkaruppan et al. [17]. Thus we consider a small solid tumour implanted in the cornea of a test animal close to the limbal vessels. Angiogenesis is quick (14–21 days) and tumour growth evolves continuously from the avascular phase, through angiogenesis to the vascular phase.

A novel feature of our model, compared to previous models, is that tumour-host interactions are active in the region while the new capillary network is forming during angiogenesis. This enables us to investigate how the coupling of tumour-host dynamics and angiogenesis influences tumour growth. To our knowledge this has not been considered in existing models, which have tended to focus on a single specific aspect of tumour development.

Tumour growth, via invasion of the surrounding host cells, and angiogenesis are multidimensional processes. By averaging the dependent variables in a plane perpendicular to the direction of motion of the vascular front it is possible to restrict attention to one spatial dimension. This direction is chosen to be parallel to the line connecting the limbus, situated at $x = 0$ and where the nearest host blood vessels are found, to the tumour centre at $x = 1$ (in dimensionless terms). We introduce independent variables t and x representing, respectively, time and spatial position in a direction parallel to that of tip growth.

Within our modelling framework we consider two types of dependent variables: those that contribute to the tumour volume and those of negligible volume. In the former category we include the healthy (host) cell density $n_1(x,t)$, the tumour cell density $n_2(x,t)$ and two components for the vasculature, namely the capillary tip density $n_3(x,t)$ and the density of the blood vessels $b(x,t)$. The nutrient, which in our case is oxygen, concentration $a(x,t)$ and TAF, which in our model is VEGF, concentration $c(x,t)$ are assumed to be of negligible volume. To formulate the model equations we combine models by Byrne and Chaplain [6] and Gatenby and Gawlinski [11]. Following [6], the deterministic modelling of the vasculature-TAF interactions is based on the fungal growth model of [9], the two processes sharing many common features, including branching, anastomosis and migration [12,17]. Based on experimental results by Sholley et al. [29], we assume that migration of the capillary tips up the gradient of VEGF concentration is the key mechanism during angiogenesis and that proliferation of the cells at the capillary tip stimulated by VEGF is secondary, and as a result, less significant. This makes our model assumptions biologically different from the modelling assumptions from [6].

Following [11] we model the tumour-host interactions via non-linear reaction-diffusion equations for the cell density. However, we assume that the normal tissue is immobile and neglect its random motion coefficient. As in [11] we assume that the tumour is unable to spread unless the surrounding healthy tissue has been diminished from its carrying capacity by, for example, increased acidity leading to death of normal cells. Thus we consider the expansion of the tumour into the adjacent tissue to depend on its composition and we model the random motion coefficient for the tumour cell density to be dependent on the density of the surrounding normal cells. Unlike [11] the equations we use for the tumour and the host cell density are coupled via the oxygen equation, rather than hydrogen ion density H^+ as a measure of the pH and acidity of the region. Oxygen is blood-borne and it controls cell proliferation and oxygen-deprived (hypoxic) death. These assumptions are based on experimental observations of tumour-host interactions in the presence and absence of oxygen [7]. The novel aspect of our model is the coupling of the equations for the cell densities and oxygen concentration with equations for the vasculature-TAF interactions. We explore the fact that when oxygen concentration in the region lowers, tumour cells (and to a lesser extent normal cells) secrete VEGF [13]. We incorporate this by assuming that VEGF is produced by the tumour and the normal cells under hypoxia. This coupling distinguishes our model from [11], from [6] and from previous models such as [8].

Combining the above ideas we arrive at the following non-dimensionalised system of equations (see [22] for details):

$$\frac{\partial n_1}{\partial t} = \underbrace{\frac{r_1\rho_1 a}{1+\rho_1 a}n_1}_{\text{proliferation}} - \underbrace{r_1 n_1^2}_{\text{crowding}} - \underbrace{\frac{R_1 n_1}{1+\rho_1 a}}_{\text{hypoxic death}} - \underbrace{c_1 n_1 n_2}_{\text{competition}} \tag{18.1}$$

$$\frac{\partial n_2}{\partial t} = \underbrace{\frac{\partial}{\partial x}\left(d_{n_2}(1-n_1)\frac{\partial n_2}{\partial x}\right)}_{\text{random motion}} + \underbrace{\frac{r_2\rho_2 a}{1+\rho_2 a}n_2}_{\text{proliferation}} - \underbrace{r_2 n_2^2}_{\text{crowding}} - \underbrace{\frac{R_2 n_2}{1+\rho_2 a}}_{\text{hypoxic death}} - \underbrace{c_2 n_1 n_2}_{\text{competition}} \tag{18.2}$$

$$\frac{\partial a}{\partial t} = \underbrace{d_a\frac{\partial^2 a}{\partial x^2}}_{\text{diffusion}} + \underbrace{hb(1-a)}_{\text{delivery by blood vessels}} - \underbrace{\frac{\lambda_1 r_1 a n_1}{1+\rho_1 a}}_{\text{consumption by host cells}} - \underbrace{\frac{\lambda_2 r_2 a n_2}{1+\rho_2 a}}_{\text{consumption by tumour cells}} \tag{18.3}$$

$$\frac{\partial c}{\partial t} = \underbrace{d_c\frac{\partial^2 c}{\partial x^2}}_{\text{diffusion}} + \underbrace{\frac{r_3}{1+\rho_1 a}n_1}_{\text{secretion by host cells}} + \underbrace{\frac{r_4}{1+\rho_2 a}n_2}_{\text{secretion by tumour cells}} - \underbrace{p_1 bc}_{\text{removal by vessels}} - \underbrace{\gamma c}_{\text{natural loss}} \tag{18.4}$$

$$\frac{\partial n_3}{\partial t} = \underbrace{d_{n_3}\frac{\partial^2 n_3}{\partial x^2}}_{\text{random motion}} - \underbrace{\frac{\partial}{\partial x}\left(\frac{\psi c}{1+\eta c}n_3\frac{\partial c}{\partial x}\right)}_{\text{chemotaxis}} + \underbrace{p_2 bc}_{\text{branching}} - \underbrace{\beta_1 n_3 b}_{\text{anastomosis}} \tag{18.5}$$

$$\frac{\partial b}{\partial t} = \underbrace{d_{n_3}\frac{\partial n_3}{\partial x}}_{\text{random motion}} - \underbrace{\frac{\psi c}{1+\eta c}n_3\frac{\partial c}{\partial x}}_{\text{snail-trail production}} + \underbrace{s_1 b(1-b)}_{\text{vessel remodelling}} - \underbrace{\delta b}_{\text{natural loss}}. \tag{18.6}$$

The corresponding initial and boundary conditions are

$$\frac{\partial n_2}{\partial x}(0,t) = 0, \quad \frac{\partial a}{\partial x}(0,t) = -hb(1-a), \quad \frac{\partial c}{\partial x}(0,t) = p_3 bc, \quad n_3(0,t) = e^{-kt}, \tag{18.7}$$

$$\frac{\partial n_2}{\partial x}(1,t) = 0, \quad \frac{\partial a}{\partial x}(1,t) = 0, \quad \frac{\partial c}{\partial x}(1,t) = 0, \quad \frac{\partial n_3}{\partial x}(1,t) = 0, \tag{18.8}$$

$$n_1(x,0) = 1 - n_2(x,0), \quad n_2(x,0) = \frac{1}{1+\exp(-\epsilon_2(x-a_2))}, \quad a(x,0) = 1, \tag{18.9}$$

$$c(x,0) = 0, \quad b(x,0) = \frac{1}{1+\exp(\epsilon_4(x-a_4))}, \quad n_3(x,0) = \frac{1}{1+\exp(\epsilon_3(x-a_3))}. \tag{18.10}$$

We make the simple modelling assumption that captures the effect of a one-off formation of capillary tips at the limbus as the condition $n_3(0,t) = e^{-kt}$, where k represents the rate of tip decrease at the limbus. The blood vessels at the limbus supply the region with oxygen and also remove the excess VEGF. For the tumour density we impose a no-flux boundary condition at $x = 0$. We assume symmetry of the tumour about its centre and hence impose no flux boundary conditions for n_2, a, c and n_3 at $x = 1$. We assume that initially some tumour cells are located at $x = 1$, the rest of the domain is filled with normal cells and that the vasculature is only present near the limbus. Initially the region is well oxygenated and no VEGF is present.

18.3 Model Simulations

We investigate, using numerical computation, the behaviour of the model in various parameter regimes. We use the NAG library routine DO3PCF which discretises the system of equations using finite differences and solves the resulting system of ordinary differential equations using backward differentiation [26]. We find that, by changing parameter values, the model can simulate a growing tumour before and after vascularisation, as well as the clearance of the tumour due to interactions with the host tissue. Qualitatively we can capture avascular tumour growth with invasion of the host cells, the migration of the neovasculature during the angiogenic process and also vascular tumour growth characterised by the tumour growing larger and invading the host cells more rapidly than its avascular counterpart.

In Fig. 18.1(a)–(e) we present numerical solutions of the equations (18.1)–(18.10) for different parameter values. We observe avascular tumour growth and tumour invasion of the host cells (see Fig. 18.1(a)); successful angiogenesis and tumour invasion of the host cells (see Fig. 18.1(b)); avascular tumour growth and tumour coexistence with the host cells (see Fig, 18.1(c)); successful angiogenesis and tumour-host coexistence (see Fig. 18.1(d)); and tumour regression during avascular growth only (see Fig. 18.1(e)). We note that changes in key model parameters (competition parameters c_1, c_2 and oxygen consumption λ_2 as well as the chemotactic parameters η, ψ) allow us to switch from one type of behaviour to another. We illustrate this in the bifurcation diagrams in Fig. 18.2(a)–(c) where parameter space is divided into distinct regions depending on the outcomes of the simulations.

Our results suggest that the success of the angiogenic process depends on the strength of tumour-host competition: only when the tumour can compete with the host cells will angiogenesis be completed (regions M and P in Fig. 18.2(a)–(b)). Thus we predict that angiogenesis must follow invasive avascular tumour growth and it is not possible for a tumour that initially regresses to then undergo angiogenesis and invade the host cells. This occurs because in our model the tumour cells are the main source of VEGF. Hence when the normal cells are dominant the tumour recedes and VEGF secretion decreases (see Fig. 18.1(e)). Tumour vascularisation is quicker when the tumour consumes larger amounts of oxygen (i.e., as λ_2 increases; see Fig. 18.3(a)). Equally, increasing λ_2, and making the region hypoxic, in Fig. 18.2(a)–(b), increases the size of the region P thus making it more likely for the tumour to invade the host cells. This suggests that tumour invasion is stronger in hypoxic conditions and this is a new prediction of our model. Combining these results we predict that hypoxic conditions, brought about by large oxygen consumption by the tumour cells, render the tumour more invasive and able to vascularise more quickly.

Successful angiogenesis, in Fig. 18.4(c)–(d), is characterised by vascular profiles that propagate from the limbal vessels towards the tumour, with increasing speed and increasing maximum density (see Fig. 18.4(c)). In addition the capillary tip profiles precede the vessel profiles (compare Figs. 18.4(c) and 18.4(d)). These are features of what is called the brush-border effect associated with successful tumour vascularisation in the experiments by Muthukkaruppan [17]. By tracking the position of a point in the wave front over time, we estimate the speed of propagation of the tips to be

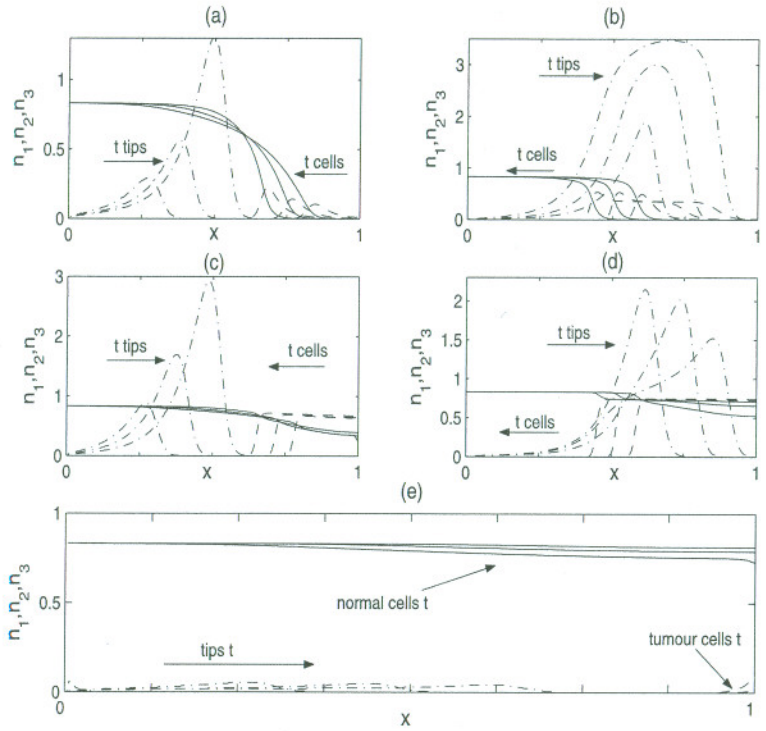

Fig. 18.1. Series of plots illustrating the types of behaviour that emerge from equations (18.1)–(18.10). The normal $n_1(-)$ and the tumour cell density $n_2(--)$ propagate as waves of normal cell regression and tumour invasion before and after successful vascularisation (a)–(d); or when the normal cells are better competitors the tumour density regresses (e) in which case angiogenesis is unsuccessful. Following successful vascularisation the tumour grows larger ((b) and (d)). During avascular tumour invasion in (a) and (c) the capillary tips $n_3(-.-)$ propagate from the limbus towards the tumour with increasing speed and increased maximum density. Post angiogenesis tip profiles propagate with constant speed and either increase to a maximum value within the tumour mass (b) or decrease towards the tumour centre (d). The results are shown at dimensionless $t = 5, 10, 15$ in (a), (c) and (e) and $t = 20, 25$ and 30 in (b) and (d). Parameter values: $r_1 = 4, \rho_1 = 8, R_1 = 1, r_2 = 10, \rho_2 = 15, R_2 = 2, d_{n_2} = 0.0007, h = 10, \lambda_1 = 0.1, r_3 = 0.1, r_4 = 10, p_1 = 10, d_c = 0.28, \gamma = 1, d_{n_3} = 0.0001, \psi = 0.8, \eta = 1.5, p_2 = 50, \beta_1 = 10, s_1 = 1, \delta = 0.25, k = 30, p_3 = 10, \epsilon_2 = 250, a_2 = 0.9, \epsilon_3 = \epsilon_4 = 250, a_3 = a_4 = 0$ and (a) $c_1 = 10, c_2 = 5, \lambda_2 = 50$; (b) $c_1 = 1, c_2 = 5, \lambda_2 = 0.5$; (c) $c_1 = 1, c_2 = 25, \lambda_2 = 50$.

approximately 0.03 in dimensionless units (or 0.11 mm day^{-1} in dimensional units) near the limbus and 0.13 in dimensionless units (or 0.4 mm day^{-1}) near the tumour in Fig. 18.4(c). This agrees with experimental measurements showing the vascular speed increasing from 0.1–0.2 mm day^{-1} near the limbus to 0.3–0.8 mm day^{-1} near the tumour [10]. Once the tumour is vascularised the speed of the vascular front becomes constant and approximately that near the limbus prior to angiogenesis. Therefore once the vessels penetrate the tumour their rate of propagation becomes constant. Furthermore the maximum density of the capillary tips either reaches a maximum value within the tumour mass (see Fig. 18.1(b)) or decreases towards the tumour centre once the tips have penetrated the tumour (see Fig. 18.1(d)). The former case occurs when the tumour is a better competitor than the host cells, whereas the latter case occurs when the tumour cells coexist with the host cells. Therefore we predict that the outcome of

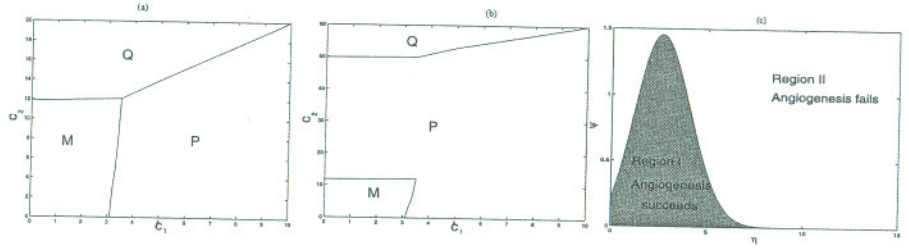

Fig. 18.2. (a)–(b) Diagram showing how the competition (c_1, c_2) parameter space can be decomposed into distinct regions depending on the long-time behaviour of the model solutions, for two different values of λ_2. In (a) $\lambda_2 = 5$ and in (b) $\lambda_2 = 50$. In regions M and P the tumour is a similar or better competitor than the normal cells, the numerical solutions evolve as travelling waves of tumour invasion of the host cells during the avascular phase followed by successful angiogenesis and vascular tumour growth. In region Q the normal cells dominate; the tumour regresses and fails to become vascularised. (c) Diagram showing the existence of a numerically calculated region where the tumour grows as avascular or vascular depending on the values of the chemotactic parameters η and ψ. This parameter space is determined with detailed numerical simulation. The rest of the parameter values are as per Fig. 18.1(a) with tumour being the better competitor and $(c_1, c_2) \in$ P from (a)–(b). Qualitatively the results are the same when $(c_1, c_2) \in$ M from (a)–(b).

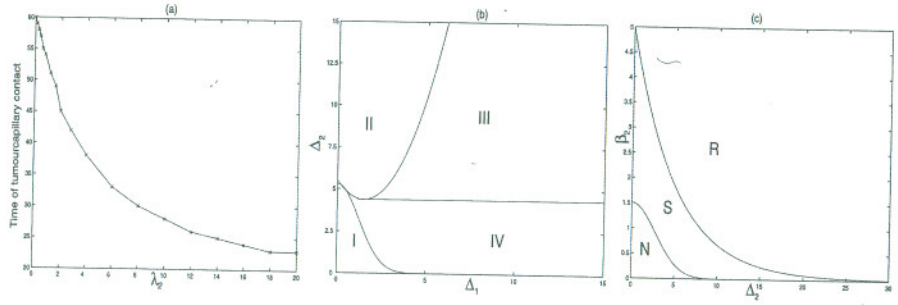

Fig. 18.3. (a) Numerically calculated decrease in the time when the tumour becomes vascularised as a function of the parameter λ_2 that controls oxygen consumption by the tumour cells. (b)–(c) Diagrams illustrating how the (Δ_1, Δ_2) and (Δ_2, β_2) parameter spaces can be decomposed into distinct regions depending on the effectiveness of an anti-proliferative therapy. In (b) in the long term, only tumour cells are killed (II), only normal cells are killed (IV), both cell types are killed (III) by the therapy, or it has no effect on tumour growth (I). In (c) the therapy is not effective in region N; the tumour regresses and is removed in region R and the tumour reaches saturated growth in region S.

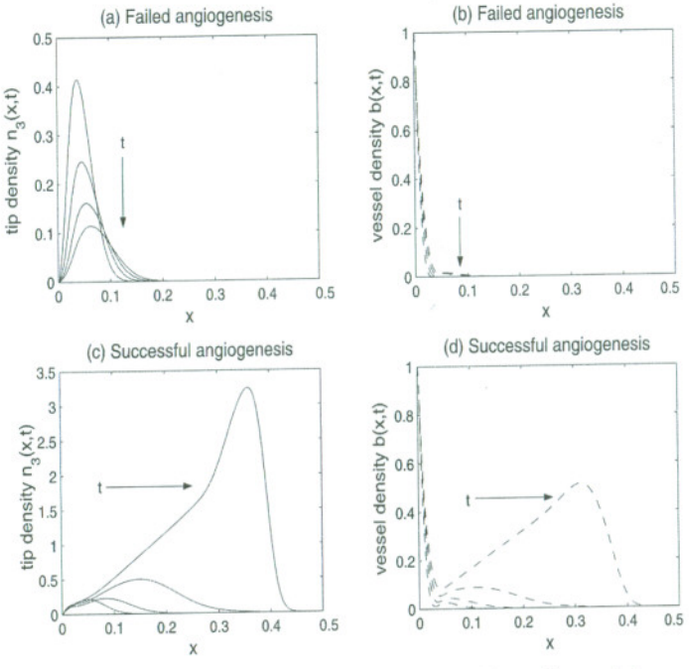

Fig. 18.4. Series of plots illustrating the profiles of the capillary tips and the vessel density during unsuccessful angiogenesis (a)–(b) and during successful angiogenesis with brush border (c)–(d). The parameters are as in Fig. 18.1(a) apart from $\gamma = 19, \eta = 50$ for (a)–(b) and $\gamma = 1$, $\eta = 1.5$ for (c)–(d). We plot the profiles at dimensionless $t = 5, 10, 15, 20$.

the tumour-host interaction affects the behaviour of the vasculature during vascular growth. A large vascular density (capillary tips in Fig. 18.1(b)) during vascular tumour growth is, in our simulations, present during successful invasion of the host tissue by the tumour cells. A small vascular density (capillary tip density in Fig. 18.1(d)) is associated with tumour-host coexistence during vascular growth.

The model also shows that angiogenesis enhances the ability of the tumour cells to invade the host tissue. For example, for the profiles depicted in Fig. 18.1(c) the tumour invasion speed increases from 0.09 (or 0.27 mm day^{-1}) to 0.105 (or 0.315 mm day^{-1}) following successful angiogenesis. In addition the tumour density is much larger following angiogenesis (compare Figs. 18.1(a) and 18.1(b)). These results suggest that in the later stages of tumour growth, following vascularisation, the tumour grows much larger and is more invasive than during the initial avascular stages of tumour growth. These observations agree with experimental observations of tumour growth *in vivo* [10].

18.4 Applications of the Model

The model (18.1)–(18.10) can be used to investigate the effect of different anti-cancer treatments. We now extend our model to include an equation for a blood-borne drug with different modes of action. For example, model simulations suggest that a tumour which in the absence of therapy invades the adjacent host tissue, when treated continuously with an anti-proliferative drug can saturate in growth or can regress. The effect of the drug in our simulations is thus similar to the effect of chemotherapeutic drugs such as doxorubicin [3] which target rapidly proliferating cells. In Fig. 18.3(b)–(c) we depict the bifurcation diagrams for the parameters that control the effectiveness of the anti-proliferative therapy: Δ_1 and Δ_2 associated with the potency of the drug on the healthy and the tumour cells and β_2 representing the rate of drug uptake by the tumour cells. We predict that the therapy is most effective when the potency on the tumour cells and the uptake of the drug by the tumour cells are large, whereas the potency on the normal cells is small.

Alternatively we study administration of a drug that destroys the vascular network. Such a drug may fall into two categories: one that targets the angiogenic stimuli (e.g., VEGF) via inhibitors such as endostatin [19] or angiostatin [20]; or a drug such as combretastatin (CAP4) [33] that directly targets the immature blood vessels. Within our model we are able to incorporate these different modes of action of the anti-vascular drug and compare the outcomes. Qualitatively the results are the same. Our simulations predict that upon administration of the anti-vascular drug tumour vascularisation can be prevented but tumour invasion of the host cells continues in this case. The tumour density resembles an avascular mass that invades with a constant speed. This is unrealistic, as we know that avascular tumours cannot grow indefinitely, and occurs because the model [11] does not properly include necrosis. Recently, an extension of the model in [11] has been proposed and shown to exhibit growth saturation [30]. A future extension of the present integrated model would be to include this new model.

When a combination of anti-proliferative and anti-vascular therapy is introduced into our model, the qualitative outcome is similar to that when only anti-proliferative therapy is applied. Tumour invasion into the host cells can either be halted and the tumour reaches a saturated growth, or tumour invasion is reversed and the tumour regresses. For more details of these and other therapeutic applications see [22] and [24].

18.5 Conclusions

We believe that the mathematical model presented here enables us to better understand the complex interactions that govern tumour growth. The continuum approach adopted in [22] allows us to make analytical predictions, for example, of wavespeed of invasion. Recently many cellular automata (CA) approaches have been developed to describe different aspects of tumour growth (see [16]). CA allows one to consider properties of individual cells but there is little in the way of mathematical theory developed for such models. Our model was the first deterministic model to study how tumour cells,

host cells and host blood vessels interact. With our results we can capture avascular followed by vascular tumour growth, as well as tumour elimination due to interactions with the host tissue. We can confirm that a vascular tumour is more aggressive and grows larger than its avascular counterpart. This agrees with *in vivo* observations of tumour growth and the modelling results presented in [4]. Furthermore we predict that it is not possible for a tumour that initially regresses to undergo angiogenesis and then invade the host cells. This may be a consequence of the fact that we do not allow for genetic mutations of the tumour cells. Our simulations also suggest that, during vascular growth, the maximum density of immature vessels within the tumour mass stays constant or decreases towards the tumour centre. In practice the situation which arises depends on the nature of the tumour-host interactions.

In terms of novel therapies, our numerical results suggest that targeting a vascular tumour with a highly potent anti-proliferative drug in combination with reducing the VEGF influence in the region (and thus preventing angiogenesis) is the most effective treatment. When the therapy only destroys the vascular network, we predict that angiogenesis can be prevented but tumour invasion will continue unaffected. We note that in our model there is continuous infusion of the drug. Questions remain as to whether such a therapy is feasible and, of course, our modelling framework does not account for the issue of side effects. A full critique of this modelling approach together with possibilities for further research are presented in [24].

Acknowledgments

This work was carried out whilst J.P. was a graduate student at the Centre for Mathematical Biology, Mathematical Institute, Oxford University and was funded by The Queen's College Studentship. J.P. also acknowledges support from The Society for Mathematical Biology Landhal Grant and the ECMTB Young Researchers Grant facilitating her to attend the meeting. H.M.B. gratefully acknowledges the support of an EPSRC Advanced Research Fellowship.

References

1. Anderson, A.R.A., Chaplain, M.A.J.: Continuous and discrete mathematical models of tumour-induced angiogenesis. Bull. Math. Biol., **60**, 857–900 (1998).
2. Arakelyn, L., Merbi, Y., Agur, Z.: Vessel maturation effects on tumour growth: validation of a computer model in implanted human ovarian carcinoma spheroids. Eur. J. Cancer, **41**, 159–167 (2004).
3. Baxter, L.T., Yuan, F., Jain, R.K.: Pharmacokinetic analysis of the perivascular distribution of bifunctional antibodies and haptens: comparison with experimental data. Cancer Res., **52**, 5838 (1992).
4. Breward, C.J.W., Byrne, H.M., Lewis, C.E.: A multiphase model describing vascular tumour growth. J. Math. Biol., **65**, 609–640 (2003).
5. Breward, C.J.W., Byrne, H.M., Lewis, C.E.: Modelling the interaction between tumour cells and a blood vessel in micro-environment within a vascular tumour. Eur. J. Appl. Math., **12**, 529–556 (2001).

6. Byrne, H.M., Chaplain, M.A.J.: Mathematical models for tumour angiogenesis-numerical simulations and non-linear wave solutions. Bull. Math. Biol., **57**, 461–486 (1995).
7. Casciari, J.J., Sotirchos, S.V., Sutherland, R.M.: Variations in tumour growth rates and metabolism with oxygen concentration, glucose concentration and extracellular pH. J. Cell. Physiol., **151**, 386–394 (1992).
8. De Angelis, E., Preziosi, L.: Advection-diffusion models for solid tumour evolution in vivo and related free boundary problems. Math. Models Methods Appl. Sci., **10**, 379–407 (2000).
9. Edelstein, L.: The propagation of fungal colonies: a model for tissue growth. J. Theor. Biol., **98**, 679–701 (1982).
10. Folkman, J.: The vascularization of tumours In: Friedberg, E.C. (ed.) Cancer Biology: Readings from Scientific American. 115–124 (1986).
11. Gatenby, R.A., Gawlinski, E.T.: A reaction-diffusion model of cancer invasion. Cancer Res., **56**, 5745–5753 (1996).
12. Gimbrone, M.A., Cotran, R.S., Leapman, S.B., Folkman, J.: Tumour growth and neovascularisation: an experimental model using rabbit cornea. J. Natl. Cancer Inst., **52**, 413–427 (1974).
13. Griffiths, L., Daches, G.U.: The influence of oxygen tension and pH on the expression of platelet-derived endothelial cell growth factor thymidine phosphorylase in human breast tumour cells *in vitro* and *in vivo*. Cancer Res., **57**, 570–572 (1997).
14. Hahnfield, P., Panigraphy, D., Folkman, J., Hlatky, L.: Tumour development under angiogenic signalling: a dynamic theory of tumour growth, treatment response and post-vascular dormancy. Cancer Res., **59**, 4770–4775 (1999).
15. Jackson, T.L., Byrne, H.M.: A mathematical model to study the effects of drug resistance and vasculature on the response of solid tumours to chemotherapy. Math. Biosci., **164**, 17–38 (2000).
16. Moreira, J., Deutsch, A.: Cellular automaton models of tumour development: a critical review. Adv. Comp. Sys., **5**, 247–267 (2002).
17. Muthukkaruppan, V.R.M., Kubai. L., Auerbach, R.: Tumour-induced neovascularisation in the mouse eye. J.Natl.Cancer Inst., **69**, 699–705 (1982).
18. d'Onfrio, A., Gandolfi, A.: Tumour eradication by anti-angiogenic therapy: analysis and extension of the model by Hahnfeldt et al. (1999). Math. Biosc., **191**, 154–184 (2004).
19. O'Reilly, M.S., Boehm, T., Shing, Y., Fukai, N., Vasios, G., Lane, W.S., Flynn, E., Birkhead, J.R., Olsen, B.R., Folkman, J.: Endostatin: an endogenous inhibitor of angiogenesis and tumour growth. Cell, **88**, 277–285, (1997).
20. O'Reilly, M.S., Holmgren, L., Shing, Y., Chen, C., Rosenthal, R.A., Moses, M., Lane, W.S., Cao, Y., Sage, E.H., Folkman, J.: Angiostatin. A novel angiogenic inhibitor that mediates the suppression of metastasis by a Lewis lung carcinoma. Cell, **79**, 315–328, (1994).
21. Orme, M.E., Chaplain, M.A.J.: Two-dimensional models of tumour angiogenesis and anti-angiogenic strategies. IMA. J. Math. Appl. Med. Biol., **14**, 189–205 (1997).
22. Panovska, J.: Mathematical modelling of tumour growth and applications for therapy, D.Phil. Thesis, Oxford University, UK (2005).
23. Panovska, J., Byrne, H., Maini, P.: A mathematical model of vascular tumour growth, (in preparation).
24. Panovska, J., Byrne, H., Maini, P.: A theoretical study of the response of vascular tumours to different types of chemotherapy, (in preparation).
25. Pettet, G.J., Please, C.P., Tindall, M.J., McElwain, D.L.S.: The migration of cells in multicell tumor spheroids. Bull. Math. Biol., **63**, 231–257 (2001).

26. Press, W.H., Teukolsky, S.A., Vetterling, W.T., Flannery, B.P.: Numerical recipes in Fortran: the art of scientific computing, 2nd edition. Cambridge University Press (1994).
27. Sherratt, J.A., Chaplain, M.A.J.: A new mathematical model for avascular tumour growth. J. Math. Biol., **43**, 291–312 (2001).
28. Sherratt, J.A., Nowak, M.A.: Oncogenes, anti-oncogenes and the immune response to cancer: a mathematical model. Proc. R. Soc. Lond., **248**, 261–271 (1992).
29. Sholley, M.M., Ferguson, G.P.: Mechanism of neovascularisation.Vascular sprouting can occur without proliferation of endothelial cells. Lab. Invest., **51**, 624–634 (1984).
30. Smallbone, K., Gavaghan, D.J., Gatenby, R.A., Maini, P.K.: The role of acidity in solid tumour growth and invasion. J. Theor. Biol., **235**, 476–484 (2005).
31. Sutherland, R.M.: Cell and environment interactions in tumour microregions: the multicell spheroid model. Science, **240**, 177–184 (1988).
32. Ward, J.P., King, J.R.: Mathematical modelling of avascular-tumour growth II: Modelling growth saturation. IMA J. Math. Appl. Med. Biol., **16**, 171–211 (1999).
33. West, C.M., Price, P.: Combretastatin A4 phosphate. Anticancer Drugs, **15**, 179–187 (2004).